JOURNAL OF Applied Polymer SCIENCE

High-performance copoly(benzimidazole-benzoxazole-imide) fibers: Fabrication, structure, and properties

Longbo Luo, Yaxin Zheng, Jieyang Huang, Ke Li, Huina Wang, Yan Feng, Xu Wang, Xiangyang Liu
State Key Laboratory of Polymer Material and Engineering, College of Polymer Science and Engineering, Sichuan University, Chengdu 610065, People's Republic of China
Correspondence to: X. Liu (E-mail: lxy6912@sina.com)

ABSTRACT: Novel high-performance copolyimide (co-PI) fibers containing benzimidazole and benzoxazole ring in the main chain were prepared by a two-step spinning via the poly(amic acid)s. Effects of the incorporated benzimidazole and benzoxazole units on the micro-structure and properties of co-PI fibers were investigated. Fourier transform infrared (FTIR) results indicated that hydrogen bonding is formed in the co-PI fibers. The co-PI fibers exhibited discernible crystallization peaks at 14°∼15° and 23°∼26° (2θ), showing crystalline-like structure. Moreover, the packing type of benzimidazole-imide units determined the macromolecules packing of co-PIs. It was amazedly found that the co-PI fibers exhibited higher tensile strength and initial modulus than those of corresponding homo-PI fibers, reaching tensile strength of 2.2–2.6 GPa, initial modulus of 99.1–113.2 GPa. The results of dynamic mechanical analysis (DMA) indicated co-PI2 fiber had a positive T_g deviation due to the presence of strong intermolecular hydrogen bonding between benzimidazole-imide and benzoxazole-imide units, which maybe lead to the effective stress transfer between benzimidazole-imide units and benzoxazole-imide units. In addition, the obtained PI fibers exhibited excellent thermal properties with the 10% weight loss temperatures under N_2 in the range of 574–585°C. © 2015 Wiley Periodicals, Inc. J. Appl. Polym. Sci. **2015**, *132*, 42001.

KEYWORDS: copolymers; crystallization; polyimides; properties and characterization

Received 3 September 2014; accepted 16 January 2015
DOI: 10.1002/app.42001

INTRODUCTION

Aromatic polyimides (PIs) have excellent thermal stability and high mechanical properties, along with good chemical resistance and electrical properties.[1–5] Because of these outstanding properties, their application in fiber, films, coating, and composites has been extensively investigated for many years.[4,6–8] However, the mechanical properties of aromatic polyimide fibers are sharply lower than those of aromatic polyamide fibers (such as Kevlar), which makes PI fibers rarely used in advanced composite materials as Kevlar fibers. For instance, Seung Koo Park, and Richard J. Farris had prepared pyromellitic dianhydride/4,4′-oxydianiline (PMDA/ODA) polyimide fibers with the tensile strength and initial modulus 0.399 GPa and 5.2 GPa, respectively.[9] In addition, as the commercial PI fiber, the tensile strength of P84 was only 0.53 GPa, whose application majored in thermal filter field.[10] Thus, as the high-performance fiber, the mechanical properties of PI fibers need to be highly enhanced.

One attempted approach to improve the mechanical properties is structural modification, such as the introduction of heterocyclic units bearing functional groups.[11] Rigid benzimidazole and benzoxazole moieties belong to this type. The benzimidazole moieties with both proton donor (—NH—) and proton acceptor (=N) hydrogen bonding sites would show strong hydrogen bonding interactions with carbonyl functionalities.[12–14] Accordingly, the copolyamide fiber ARMOS created by Russian researchers contains the benzimidazole moieties, and the mechanical properties of ARMOS fibers are superior to those of Kevlar fibers.[15,16] In addition, those polymers containing benzoxazole moieties, such as polybenzoxazoles (PBOs), usually display superior mechanical properties as well as excellent thermal stability and good environmental resistance.[17–20]

Thus, the incorporation of benzimidazole or benzoxazoles moieties into the polyimide main chains is expected to improve the mechanical, thermal and adhesive properties by many researchers.[2,11,21–28] Qingming Xia *et al.* synthesized and prepared the high-performance PI films based on 6,4′-diamino-2-phenylbenzimidazole. The obtained poly(benzimidazole-imide) films possessed good mechanical properties of tensile strength of 222–232 MPa and modulus of 3.1–5.6 GPa.[2] Guanqun Gao *et al.* prepared a series of copolyimide (co-PI) fibers containing benzimidazole moieties in the polyimide main chains, when the diamine ratio of 2-(4-aminophenyl)−5-aminobenzimidazole was

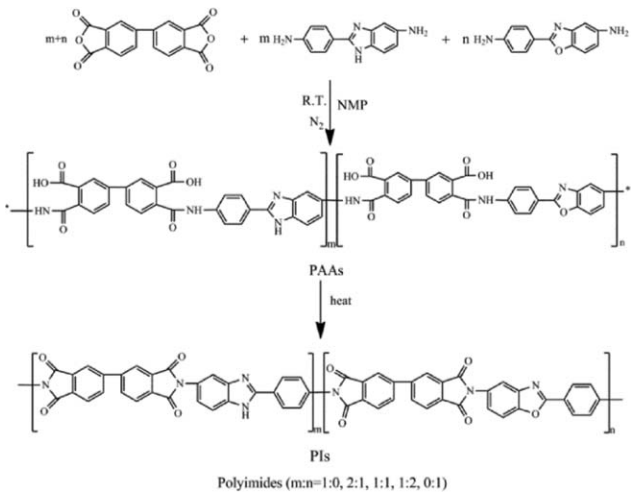

Scheme 1. Synthesis of polyimides.

70%, the tensile strength reached 1.53 GPa, which was almost three times over that of the PMDA/ODA PI fibers.[29] Zhuang *et al.* prepared the PI films containing benzoxazole moieties with tensile strength of 233.64–325.79 MPa.[11]

In our previous article,[27] the homopolyimide (homo-PI) fibers containing benzimidazole and containing benzoxazole were prepared and the crystallization behavior of two fibers was studied. In this paper, the benzimidazole and benzoxazole rings were introduced into the backbone of PIs via copolymerization in an attempt to obtain new PI fiber with excellent mechanical properties and thermal properties. When the ratio is 1 : 1, the co-PI fiber have the highest tensile strength of 2.6 GPa and initial modulus of 113.2 GPa and this value of tensile strength is superior to that of Kevlar 49®.[30] Moreover, the co-PI fibers exhibits excellent thermal properties with the 10% weight loss temperatures under N_2 in the range of 574–585°C. The new high-performance co-PI fibers will have potential application in fiber-reinforced composites.

EXPERIMENTAL

Materials

N-methyl-2-pyrrolidone (NMP) was obtained from Shanghai Qunli Chemical Company, and was distilled over P_2O_5 under reduced pressure before use. 3,3′,4,4′-Biphenyltetracarboxylic dianhydride (BPDA) was obtained from Changzhou Sunlight Medical Raw Material, China and was dried in an oven at 200°C for 10 h before use. 5-Amino-2-(4-aminobenzene) benzoxazole (BOA) and 5(6)-amino-2-(4-aminobenzene)benzimidazole (PABZ) were obtained from Changzhou Sunlight Medical Raw Material, China and used as received.

Synthesis of Poly(amic acid)s

The polyamic acids (PAAs) were prepared by mixing equimolar amounts of dianhydride and diamine dissolved in NMP under dried nitrogen atmosphere. For the polymerization, the mole ratios of PABZ and BOA were 0 : 1, 1 : 2, 1 : 1, 2 : 1, and 1 : 0, denoted as homo-PIa, co-PI1, co-PI2, co-PI3, and homo-PIb, respectively. Detailed synthesis routes have been described previously.[27] The solid content of PAA solutions were 12–14%.

Preparation of PI Fibers

The PAA solutions were filtrated and degassed at reduced pressure for 24 h before use. The PAA fibers were prepared by wet spinning. And the as-spun PAA fibers were drawn 2.4–3.0 times. Immediately after drawing, the fibers were washed by deionized water and then dried under even vacuum at 60°C for 5 h. In the second stage, the fibers were obtained by thermal imidization of PAA fibers under 0.3cN/dT tension during the heating at 6–8°C/min to 420°C for 10 min. Scheme 1 shows the synthetic process and the chemical structure of the polyimides and Scheme 2 is flow process diagram of wet spinning.

Characterization

The intrinsic viscosity of PAA solution was measured with an ubbelohde viscometer in 0.5 dL/g NMP at 30°C. Mechanical properties of the fibers were measured on YG001A-1 Fiber Electronic Strength Tester with a strain rate of 5 mm/min. The fixture span was 20 mm. One-dimensional wide angle X-ray diffraction (1D-WAXD) analysis of PI fibers was carried out on a Philips X'Pert PRO MPD. X-ray diffraction measurements were taken from the reflection mode at room temperature, using Ni-filtered Cu Kα radiation operated at 40 kV × 40 mA. Two-dimensional Wide angle X-ray diffraction (2D-WAXD) patterns of the fibers were collected on a Bruker D8 Discover with VÅNTEC-500 detectors with patented Mikrogap. The *d*-spacing of each diffraction peak was calculated using the Bragg equation. Fourier transform infrared (FTIR) spectra of PI fibers were measured at a Nicolet Magna 650 spectroscope in the range 4000–400 cm^{-1}. The frequency scale was internally calibrated with a reference helium–neon laser to an accuracy of 0.2 cm^{-1}. Dynamic mechanical analysis (DMA) was performed on a TA Q800 instrument under N_2 atmosphere at a heating rate of 10°C/min in the range of 50–550°C and the load frequency was 1 Hz. Thermogravimetric analysis (TGA) was performed using TA Instrument TGA-2950 under N_2 atmosphere at a heating rate of 10°C/min in the range of 50–800°C. Skin and fractured morphologies of the fibers were observed on a JEOL JSM-5900LV SEM. Molecular simulation was determined with Dmol3 software embedded in Material Studio 4.0 (Accelrys, USA) package on the basis of density function theory (DFT).

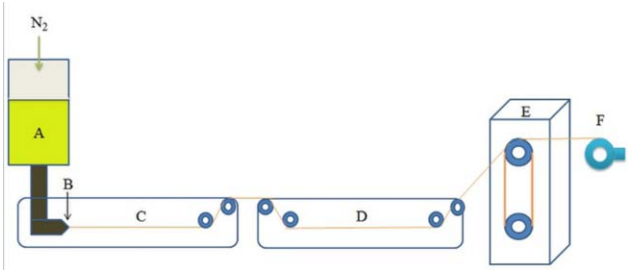

Scheme 2. Flow process diagram of wet spinning. A, spinning solution; B, a spinning spinneret with 50 holes; C, the first coagulation bath with a mixture solution of water and NMP (60/40, v/v); D, the second coagulation bath with a mixture solution of water and NMP (80/20, v/v); E, vertical washing bath, water; F, taking up roller. [Color figure can be viewed in the online issue, which is available at wileyonlinelibrary.com.]

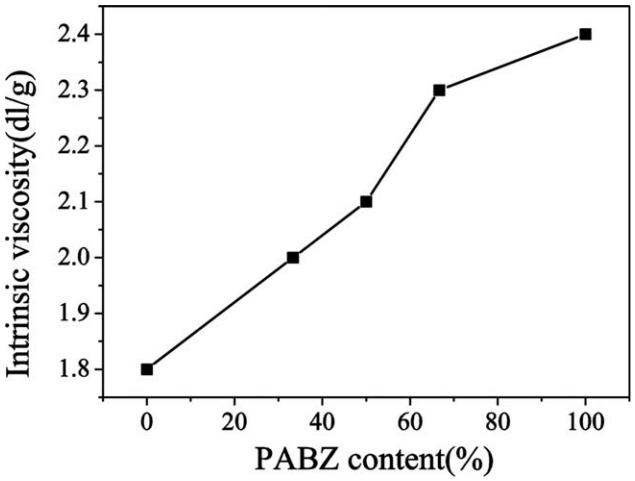

Figure 1. The relationship between intrinsic viscosity and PABZ content.

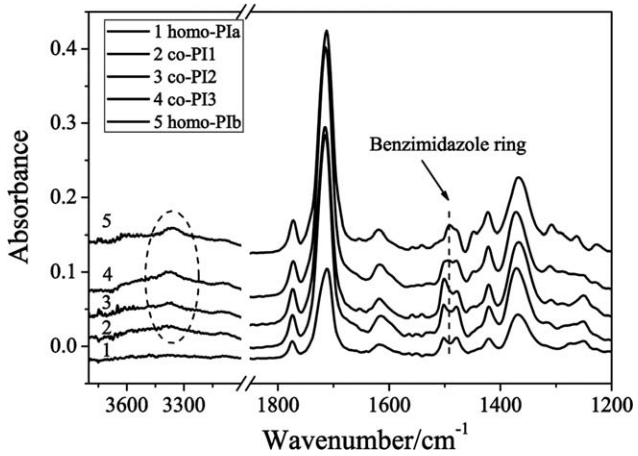

Figure 2. The FTIR profiles of homo-PIa, homo-PIb and three co-PI fibers.

RESULTS AND DISCUSSION

The Intrinsic Viscosity of Polyamic Acid

Generally, the intrinsic viscosity of PAA is used to characterize indirectly the molecular weight.[10] Figure 1 shows the relationship between the intrinsic viscosity of PAA and the PABZ content. With the increase of the PABZ content, the intrinsic viscosity value of PAA increases from 1.8 to 2.4 dL/g. This result indicates that PABZ is more favorable to obtain high molecular weight of polyimide. The charge density was calculated with Material Studio 4.0 and the result is shown in Scheme 3. Obviously, both PABZ and BOA are the asymmetry diamine monomer and the charge density of PABZ is larger than that of BOA, which leads to higher reaction reactivity with dianhydride.

Chemical Structure and Hydrogen Bonding Interactions

The FTIR results of five samples of the PI fibers are shown in Figure 2. In the region of 1800–1200 cm^{-1}, the characteristic absorption band of the imide ring are observed at about 1774 cm^{-1}(the symmetric stretching of the imide carbonyls $\nu s_{C=O}$), 1711 cm^{-1}(the asymmetric stretching of the imide carbonyls $\nu as_{C=O}$) and 1360 cm^{-1}(the stretching of C—N νs_{C-N}), respectively.[31,32] Those results indicate that the homo- and co-PI fibers were successfully prepared.[33,34] The homo-PIb and three co-PI fibers show the characteristic absorptions of benzoxazole at 1250 cm^{-1} (Ar-C-O asymmetric stretching[11]), suggesting that the benzoxazole moieties have been successfully incorporated into the main chains. The characteristic absorptions of benzimidazole at 1308 cm^{-1} (imidazole ring breathing mode[11]) are shown in homo-PIb and co-PI fibers, indicating the presence of the benzimidazole moieties. In addition, the stretching of the benzimidazole ring is at about 1490cm^{-1}.[35]

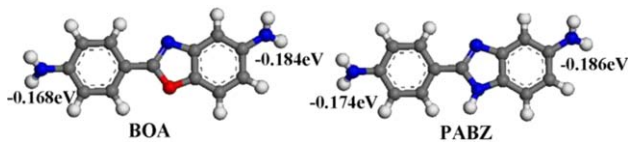

Scheme 3. Charge density of BOA and PABZ calculated by DMol3 software embedded in Material Studio 4.0. [Color figure can be viewed in the online issue, which is available at wileyonlinelibrary.com.]

With the increase of PABZ content, the intensity of the peak at 1490cm^{-1} increases.

There is a broader peak at about 3260 cm^{-1}~3500 cm^{-1} and the intensity of —NH— band increases simultaneously with an increase in PABZ content, which indicates that the introduction of benzimidazole units forms hydrogen bonding interactions between the PI chains. It is well established that the carbonyl groups of polyimide act as proton acceptors. The position of the peak of $\nu s_{C=O}$ will change when hydrogen bonds formed between —NH— of benzimidazole and C═O of imide, as shown in Figure 3. the imide C═O symmetric stretching band at 1774 cm^{-1} obviously shifts to the lower wavenumbers with increase in PABZ content, which indicates that the C═O bands of imide groups participates in the formation of hydrogen banding and the hydrogen bonding interactions enhances with the increase of the content of benzimidazole units.[24]

Morphology and Micro-Structure

The skin and fracture morphologies of the homo-PI and co-PI fibers were studied by SEM, as shown in Figure 4. Five PI fibers have a little rough surface and a lot of short microfibrils with

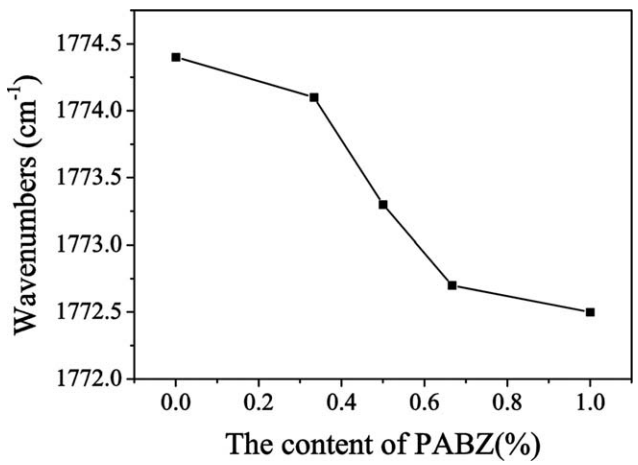

Figure 3. Band positions of C═O stretching as a function of the content of PABZ.

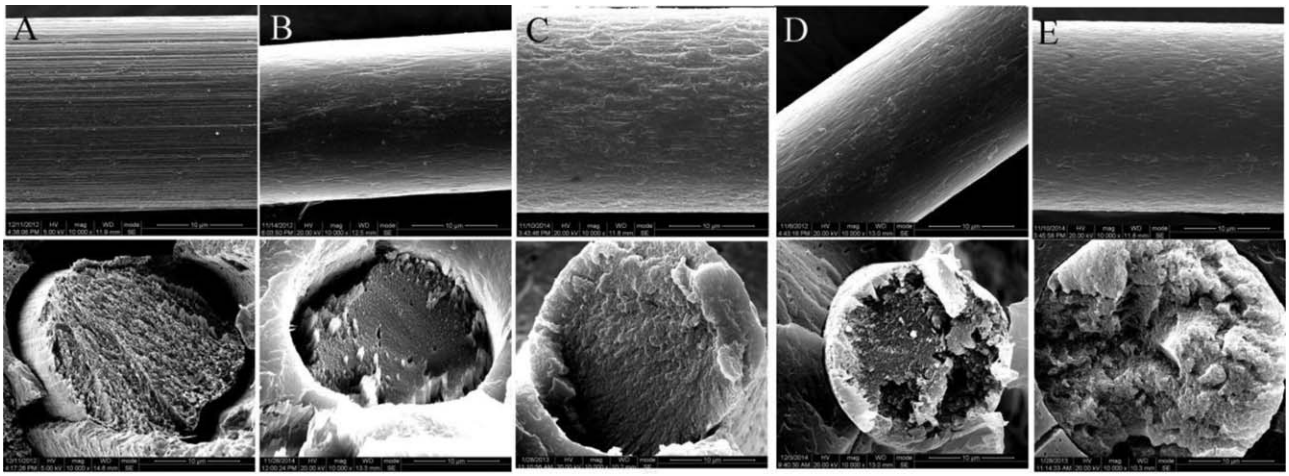

Figure 4. The skin and fracture morphologies of the homo-PI and co-PI fibers.

pores and cavities. The cross-sections of five kinds of PI fibers are round and voids free, and yet there is no obvious "skin-core" structure.

The aggregation structure of the PI and co-PI fibers was measured by 1D and 2D WAXD, as shown in Figures 5 and 6, respectively. All the diffraction peaks were deconvoluted and fitted with Gaussian broadening functions on a single baseline to estimate the central peak positions. In the equatorial directions from Figure 5, the homo-PIa fiber exhibits three discernible peaks at 14.6°, 17.0°, and 22.0° (2θ) with *d*-spacing values of 6.0, 5.2, and 4.0Å, respectively. As mentioned in previous articles,[11,36] the more intensive peak of 14.6° (2θ) correspond to the "side to side" packing of benzoxazole rings, and the peak of 22.0° (2θ) is assign to the "π–π stacking" of aromatic of heterocyclic rings. In addition, the peak of 17.0° with *d*-spacing values of 5.2 Å can be assign to interchain order packing.[37] However, the homo-PIb fiber has two crystalline peaks at 15.0° and 24.5° with *d*-spacing values of 5.9 Å and 3.6 Å, respectively, which is reported in the previous articles.[27] Similarly, the peak of $2\theta = 15°$ should be assign to "side to side" packing of benzimidazole rings, and the peaks of 24.5° (2θ) is assign to the "π–π" stacking. The former peak at small angle region is very sharp and intensive, but the latter peak at larger angle region is very weak, which indicates that "side to side" packing of benzimidazole rings is more ordered in homo-PIb. It is interesting that the $d_{spacing}$ of "side to side" and "π–π" stacking of homo-PIb are lower than those of homo-PIa. The lower value of $d_{spacing}$ may attribute to hydrogen bonding interactions in homo-PIb chains. However, the WAXD profile of three co-PI fibers are similar with homo-PIb fiber. They only exhibit "side to side" packing at about 15° and "π–π" stacking at 23∼26°, even if co-PI1 has 2/3 benzoxazole-imide units. In our previous article,[27] we reported that the hydrogen bonding interactions between —NH— of benzimidazole units and C═O of imide units hindered the integrity of the arrangements of segments. So the hydrogen bonding interaction between —NH— of benzimidazole units and C═O of imide units could reduce the degree of order of the whole macromolecular chains in co-PIs but improve the order of the "side to side" packing relative to that of homo-PIa. The high degree of order of the whole macromolecular chains be in favor of high-performance PI fibers.

In addition, there are two peaks at about 23.5° and 26°, respectively. They represent one type of "π–π" stacking without hydrogen bonding interactions and another type of "π–π" stacking with hydrogen bonding interactions, respectively. So the "π–π" stacking of co-PI chains improves relative to that of homo-PIb due to the presence of benzoxazole-imide units.

In the meridional directions, as shown in Figure 6, all of the obtained PI fibers exhibit an obvious arc at about 12.2°, indicating that the extension of macromolecules of PI containing benzimidazole or benzoxazole rings in the main chain is identical. This is due to the similar structure of benzimidazole and benzoxazole units. Because of the similar structure of benzimidazole and benzoxazole units, the co-PIs show the similar order packing of homo-PIb and will have fewer defects in order crystalline domain, which is different with other co-PIs. For example, Chaoqing Yin and coworkers[38] prepared the co-PI fibers containing benzimidazole and amide units. When the content of amide units was over 30%, the reflections corresponding to homo-PIb fibers completely disappeared, indicating the gradually loss of the lateral packing order. In addition, the periodic layer lines observed for the homopolyimide became non-periodic in the fiber diagrams of the co-PIs.[39,40] However, the extension of macromolecules of homo-PIa and homo-PIb are identical in crystalline domain. The co-PIs containing benzimidazole and benzoxazole units can exhibit the periodic layer lines.

To crystal face (hkl), the degree of orientation in crystalline region can be assessed with $<\cos 2\psi>_{hkl}$, which is calculated with the formula[41]

$$<\cos^2\psi>_{hkl} = \frac{\int_0^{\pi/2} I(\psi)\cos^2\psi \sin\psi\, d\psi}{\int_0^{\pi/2} I(\psi)\sin\psi\, d\psi}.$$

In this formula, ψ represents azimuthal angle, and $I(\psi)$ represents scanning intensity at ψ angle. A representative azimuthal

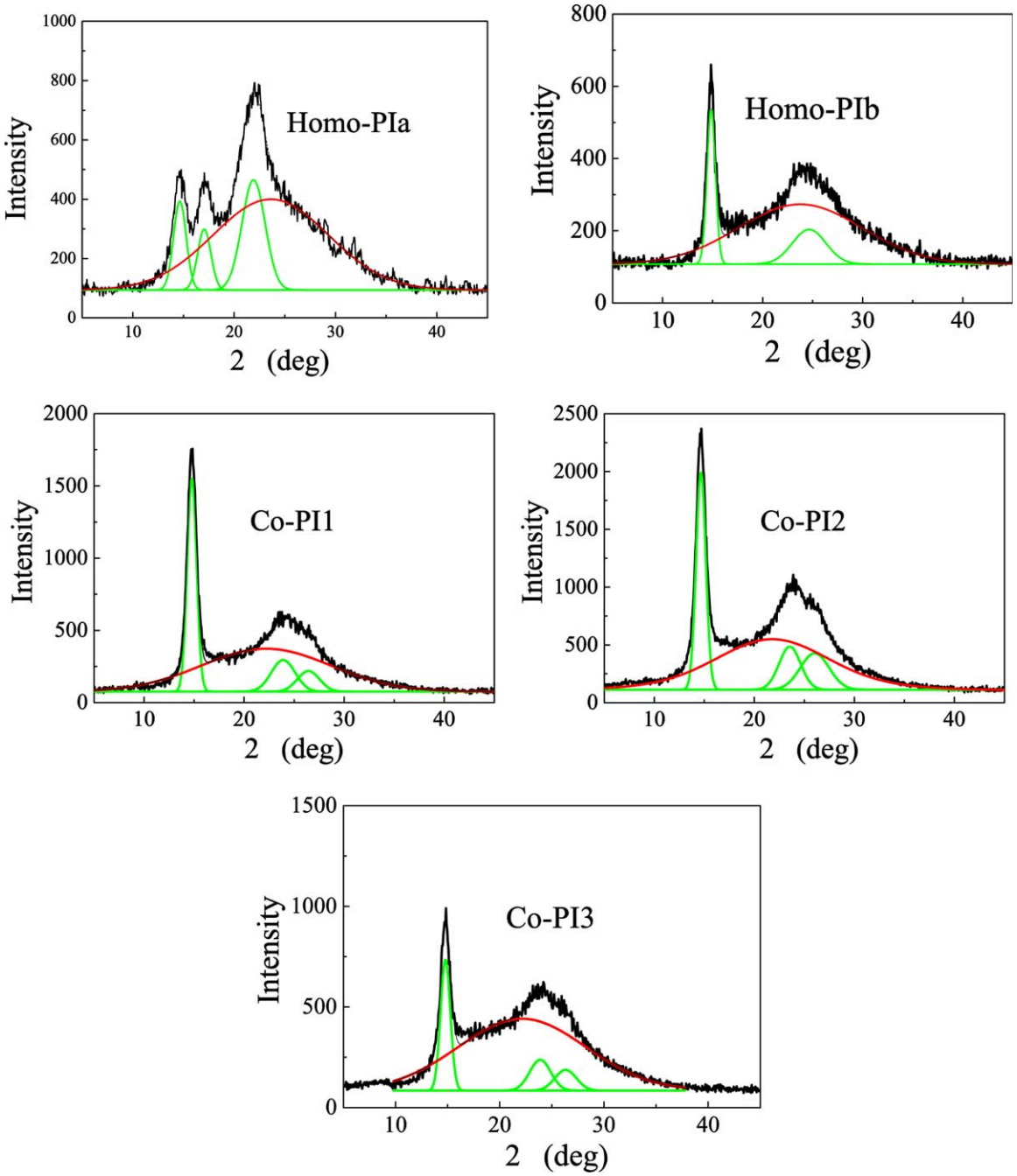

Figure 5. The 1D WAXD of (a) homo-PIa, (b) homo-PIb, (c) co-PI1, (d) co-PI2, (e) co-PI3 in the equatorial directions. [Color figure can be viewed in the online issue, which is available at wileyonlinelibrary.com.]

intensity profile of reflection at 15° obtained from co-PI2 fibers at about 15° is shown in Figure 7.

In common, f_2 is defined as Herman's orientation function, and determined with Herman Formula $f_2 = \frac{3<\cos^2\psi>-1}{2}$.[41] $<\cos 2\psi>_{hkl}$ and f_2 of five PI fibers at about 15° in the 2D-WAXD are listed in Table II. The crystalline orientation of homo-PIa, co-PI1, co-PI2, co-PI3, and homo-PIb PI fibers (calculated with above equation) are 0.81, 0.81, 0.78, 0.73, and 0.79, respectively. The co-PI3 fibers show the lower crystalline orientation, which leads to lowest tensile strength in the co-PI fibers from the results of Mechanical properties.

The Glass-Transition Temperature and Hydrogen Bonding

The glass-transition temperatures (T_gs) of PI fibers were characterized by DMA and the DMA curves of homo-and co-PI fibers are shown in Figure 8. The values of storage modulus of three co-polyimide fibers are above 60N/T and higher than those of two homo-polyimide fibers. It is indicated that co-PI fibers have better mechanical properties. Regarding the peak temperature in the tan δ curve as T_g, homo-PIa fiber exhibits the lowest value of T_g of 292°C, and homo-PIb fiber exhibits the highest value of T_g of 351°C. The values of T_gs of co-PI1, co-PI2 and co-PI3 fibers are 312°C, 327°C and 330°C, respectively. The

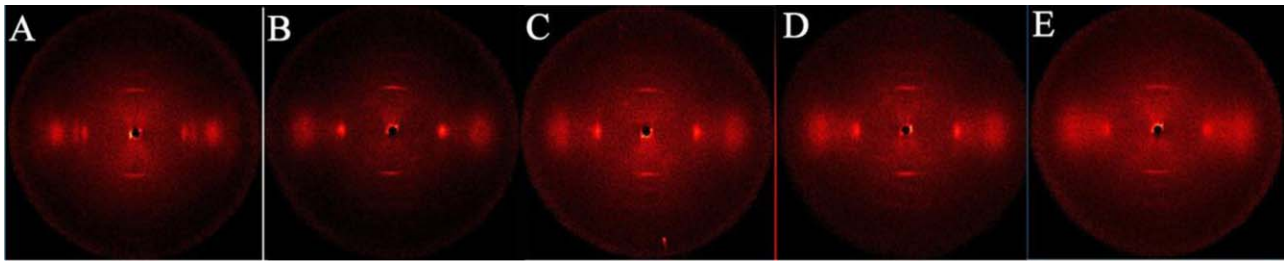

Figure 6. The 2D-WAXD profile of (a) homo-PIa, (b) homo-PIb, (c) co-PI1, (d) co-PI2, and (e) co-PI3 PI fibers, the direction of the fiber axis was vertical. [Color figure can be viewed in the online issue, which is available at wileyonlinelibrary.com.]

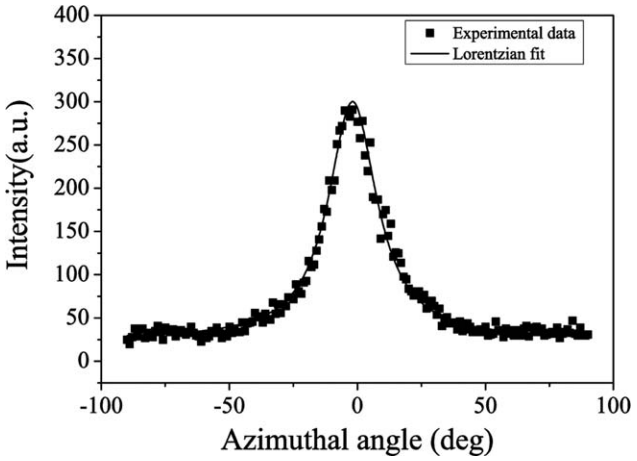

Figure 7. A representative azimuthal intensity I(ψ) profile of the "side to side" packing reflection and its Lorentzian fit overlaid with the azimuthal intensity data obtained from co-PI2. The dots represent the experimental data and the solid line corresponds to the Lorentzian fit.

values of T_gs increased with the increase of PABZ content due to the enhancement of hydrogen bonding interactions.[24]

Kwei equation[42,43] describes the effect of hydrogen bonding interactions on T_g between polymers or a copolymer as shown in eqs. (1), (2):

$$T_g = \frac{W_1 T_{g1} + kW_2 T_{g2}}{W_1 + kW_2} + qW_1 W_2 \quad (1)$$

where W_1 and W_2 are weight fractions of the components, T_{g1} and T_{g2} represent the component glass-transition temperatures. q is a parameter corresponding to the hydrogen bonding strength in the copolymers, k is the ratio of thermal expansion coefficients of two components in the liquid and glass states differences, assuming $k = 1$. The actual T_gs of co-PI fibers and theoretical T_gs calculated by Gordon-Taylor equation[44] as shown in Figure 9. The T_gs of co-PI1 and co-PI3 fibers shows no deviation, and $q \approx 0$. However, the T_g of co-PI2 fiber shows a positive deviation, and $q = 22$, which indicates strong hydrogen bonding interactions exist between benzimidazole-imide and benzoxazole-imide units of co-PI2, as shown in Scheme 4.

Mechanical Properties

The mechanical properties of single fiber of homo-PIs and co-PIs are tested and the results are shown in Table I. The tensile strength, initial modulus and elongation at break of the copoly(benzimidazole-benzoxazole-imide) fibers are in the range of 2.2–2.6 GPa, 99.1–113.2 GPa, and 3.1–3.5%, respectively, which indicates that the mechanical properties of the obtained co-PI fibers are superior. Moreover, the co-PI fibers exhibit higher tensile strength and initial modulus than those of the corresponding homo-PIa and homo-PIb fibers. This result is consistent with the studies of other researchers.[8,45,46] Sukhanova and coworkers[45] prepared homo- and co-PI fibers containing pyrimidine rings and also found that the tensile properties of co-PI fibers were better than those of homopolyimides. Haoqing Hou *et al.*[46] made electrospun co-PI nanofibers based on 3,3′,4,4′-biphenyl-tetracarboxylic dianhydride (BPDA), biphenylamide (BPA), and ODA. Their results showed the tensile strength of

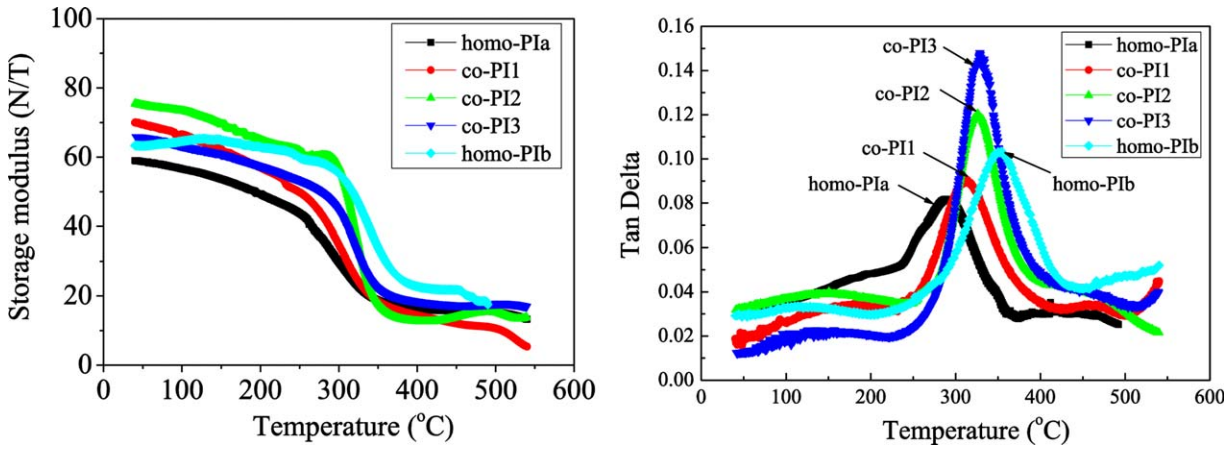

Figure 8. The DMA curves of homo-and co-PI fibers. [Color figure can be viewed in the online issue, which is available at wileyonlinelibrary.com.]

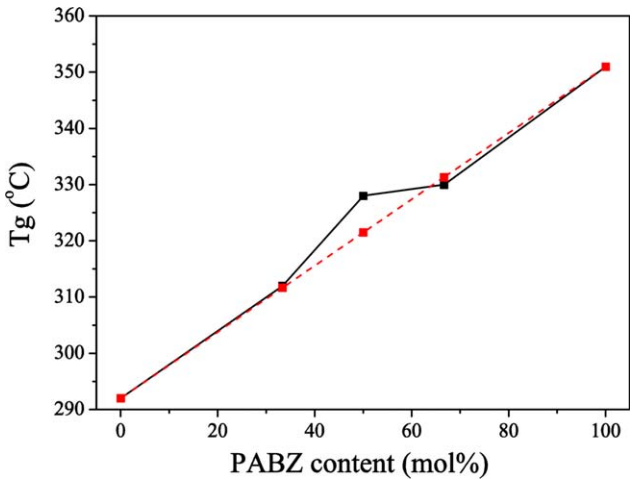

Figure 9. Variation of glass-transition temperature (T_g) with PABZ content (mol %) of the co-PI fibers. The solid line is experimentally obtained and the dotted line is calculated from the Gordon-Taylor equation. [Color figure can be viewed in the online issue, which is available at wileyonlinelibrary.com.]

the co-PI nanofiber belt with BPA/ODA ratio of 40/60 were 1.1 ± 0.1 GPa compared to 459 ± 36 MPa for BPDA/ODA homo-PI as well as 384 ± 18 MPa for BPDA/BPA homo-PI. Sukhanova and coworkers considered that the improvement in fiber modulus and tensile strength of the co-PI fibers could be attribute to the microblock structure on the X-ray level and composed morphology on the macro level.[45] In general, the high-performance PI fibers possess rigid-rod structures and the main problem in their application is the brittleness, which results in low strength. So the general idea of molecular design for fiber-forming PI is creating the co-PIs as the possible way of the development of new materials with high strength.[47,48] In our obtained co-PI fibers, the values of elongation of co-PI1 and co-PI2 fibers are higher than those of corresponding homo-PI fibers, which indicate the designed co-PIs would improve the toughness of PI fibers and delay fractures.

Furthermore, when the content of PABZ is 0.5, the tensile strength of co-PI2 fibers is highest. In our design co-PIs, the hydrogen bonding interactions and the value of T_g increase with the increase of PABZ content. However, the stronger hydrogen bonding interactions decrease the order of macromolecular of PIs.[27] So the balance is very significant in the hydrogen bonding interactions and the order of the macromolecular. In addition, only the T_g of co-PI2 fiber shows a positive deviation. This indicates strong hydrogen bonding interactions exist between benzimidazole-imide and benzoxazole-imide units of co-PI2, which maybe lead to the effective stress transfer between benzimidazole-imide units and benzoxazole-imide units. So this may be the reason that co-PI fibers show the highest tensile strength and modulus.

Table I. The Mechanical Properties of Single Fiber of Homo-PIs and co-PIs

Sample	Tensile strength (GPa)	Initial modulus (GPa)	Elongation (%)
Homo-PIa	2.0	95.6	3.1
Co-PI1	2.4	106.0	3.3
Co-PI2	2.6	113.2	3.5
Co-PI3	2.2	99.1	3.1
Homo-PIb	2.1	102.8	3.1

Table II. Results of $<\cos 2\psi>_{hkl}$ and f_2 in Crystalline Region

	R^{2a}	$<\cos^2\psi>$	f_2
Homo-PIa	0.98	0.87	0.81
Co-PI1	0.98	0.87	0.81
Co-PI2	0.98	0.85	0.78
Co-PI3	0.97	0.82	0.73
Homo-PIb	0.97	0.86	0.79

[a] $R2$ (coefficient of determination) is the measure of closeness of a regression to the data, where $R2 = 1$ is a perfect fit. Specifically, it is the covariance divided by the product of the sample standard deviations.

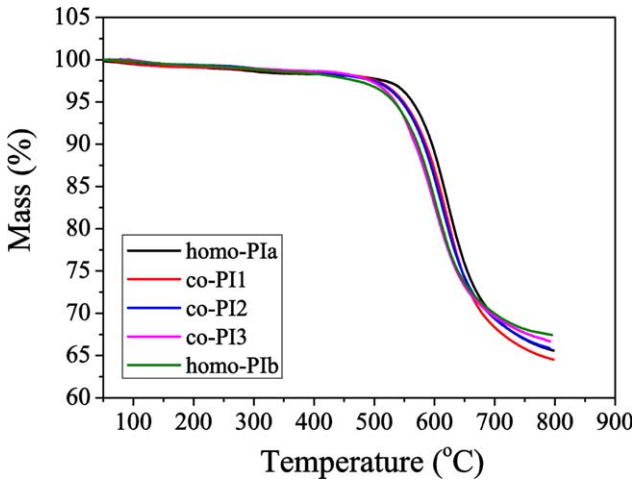

Figure 10. The TGA curves of polyimide fibers. [Color figure can be viewed in the online issue, which is available at wileyonlinelibrary.com.]

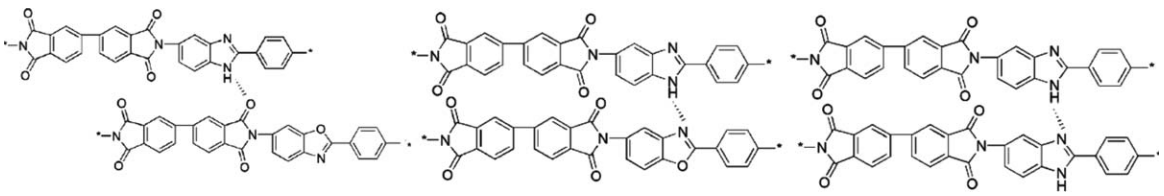

Scheme 4. Hydrogen bonding interactions between benzimidazole-imide and benzoxazole-imide units of co-PI2.

Table III. The TGA Result of PIs

Samples	$T_{5\%}$ (°C)	$T_{10\%}$ (°C)	R_w (%)
Homo-PIa	564	597	65.5
Co-PI1	548	585	64.5
Co-PI2	546	582	65.9
Co-PI3	536	574	66.7
Homo-PIb	532	572	67.5

Thermal Stability

The thermal stability of copoly(benzimidazole-benzoxazole-imide) fibers was investigated with TGA and the results are tabulated in Figure 10 and Table III. The thermal stability of the series of PI fibers is very excellent. All of the co-PI fibers have a 5% weight loss temperature in the range of 536–548°C and the 10% weight loss temperatures are in the range of 572–585°C.

CONCLUSIONS

Novel co-PI fibers containing benzimidazole and benzoxazole units in the main chain were prepared by wet spinning. All of the obtained PI fibers show ordered arrangement of the molecular chains and the packing type of benzimidazole-imide units determines the macromolecules packing of co-PIs. The introduction of PABZ containing benzimidazole moieties into the PI backbone reduces interchain packing regularity. The co-PI fibers exhibit extremely high tensile strength (2.2–2.6 GPa) and initial modulus (99.1–113.2 GPa) and the co-PI fibers exhibited higher tensile strength and initial modulus than those of the corresponding homo-PI fibers. The designed co-PIs would improve the toughness of PI fibers and delay fractures. When the content of benzimidazole is 0.5, the tensile strength of co-PI fibers reaches the highest. In addition, the co-PI fibers have good thermal properties. The 10% weight loss temperatures of the PI fibers under N_2 are in the range of 572–585°C.

ACKNOWLEDGMENTS

This work was supported by the National Natural Science Foundation of China (Grant No. 50973073) and financially supported by State Key Laboratory of Polymer Materials Engineering (Grant No. sklpme2014-2-04). The authors acknowledge Analytical & Testing Centre Sichuan University, P. R. China for characterization.

REFERENCES

1. Zhang, Q.-H.; Dai, M.; Ding, M.-X.; Chen, D.-J.; Gao, L.-X. *Eur. Polym. J.* **2004**, *40*, 2487.
2. Xia, Q.; Liu, J.; Dong, J.; Yin, C.; Du, Y.; Xu, Q.; Zhang, Q. *J. Appl. Polym. Sci.* **2013**, *129*, 145.
3. Li, B.; Pang, Y.; Fan, C.; Gao, J.; Wang, X.; Zhang, C.; Liu, X. *J. Appl. Polym. Sci.* **2014**, 131.
4. Malay, K.; Ghosh, K. L. M. Polyimides: Fundamentals and Applications; CRC Press: New York, **1996**.
5. Mehdipour-Ataei, S.; Akbarian-Feizi, L. *Chin. J. Polym. Sci.* **2011**, *29*, 93.
6. Sroog, C. *Prog. Polym. Sci.* **1991**, *16*, 561.
7. Yao, J.; Luo, L.; Wang, X.; Li, K.; Huang, J.; Gao, J.; Li, B.; Wang, H.; Zhang, C.; Liu, X. *J. Polym. Res.* **2014**, *21*, 1.
8. Niu, H.; Huang, M.; Qi, S.; Han, E.; Tian, G.; Wang, X.; Wu, D. *Polymer* **2013**, *54*, 1700.
9. Park, S. K.; Farris, R. J. *Polymer* **2001**, *42*, 10087.
10. Luo, L.; Pang, Y.; Jiang, X.; Wang, X.; Zhang, P.; Chen, Y.; Peng, C.; Liu, X. *J. Polym. Res.* **2012**, *19*, 1.
11. Zhuang, Y.; Liu, X.; Gu, Y. *Polym. Chem.* **2012**, *3*, 1517.
12. Guerra, G.; Choe, S.; Williams, D. J.; Karasz, F. E.; MacKnight, W. J. *Macromolecules* **1988**, *21*, 231.
13. Ahn, T.-K.; Kim, M.; Choe, S. *Macromolecules* **1997**, *30*, 3369.
14. Yu, J.; Ree, M.; Shin, T.; Wang, X.; Cai, W.; Zhou, D.; Lee, K.-W. *Polymer* **2000**, *41*, 169.
15. Levchenko, A. A.; Antipov, E. M.; Plate, N. A.; Stamm, M. *Macromol. Symp.* **1999**, pp 145.
16. Perepelkin, K.; Machalaba, N.; Kvartskheliya, V. *Fibre Chem.* **2001**, *33*, 105.
17. Chae, H. G.; Kumar, S. *J. Appl. Polym. Sci.* **2006**, *100*, 791.
18. Kitagawa, T.; Ishitobi, M.; Yabuki, K. *J. Polym. Sci., Part B: Polym. Phys.* **2000**, *38*, 1605.
19. Qian, J.; Wu, J.; Liu, X.; Zhuang, Q.; Han, Z. *J. Appl. Polym. Sci.* **2013**, *127*, 2990.
20. Naito, K. *J. Appl. Polym. Sci.* **2013**, *128*, 1185.
21. Liu, X.; Gao, G.; Dong, L.; Ye, G.; Gu, Y. *Polym. Adv. Technol.* **2009**, *20*, 362.
22. Wang, S.; Zhou, H.; Dang, G.; Chen, C. *J. Polym. Sci., Part A: Polym. Chem.* **2009**, *47*, 2024.
23. Liu, J.; Zhang, Q.; Xia, Q.; Dong, J.; Xu, Q. *Polym. Degrad. Stab.* **2012**, *97*, 987.
24. Guangliang, S.; Yu, Z.; Daming, W.; Chunhai, C.; Hongwei, Z.; Xiaogang, Z.; Guodong, D. *Polymer* **2013**, *54*, 2335.
25. Song, G.; Wang, S.; Wang, D.; Zhou, H.; Chen, C.; Zhao, X.; Dang, G. *J. Appl. Polym. Sci.* **2013**, *130*, 1653.
26. Zhuang, Y.; Gu, Y. *J. Polym. Res.* **2013**, *20*, 1.
27. Luo, L.; Yao, J.; Wang, X.; Li, K.; Huang, J.; Li, B.; Wang, H.; Liu, X. *Polymer* **2014**, *55*, 4258.
28. Yue, Z.; Cai, Y.-B.; Xu, S. *J. Polym. Res.* **2014**, *21*, 1.
29. Gao, G.; Dong, L.; Liu, X.; Ye, G.; Gu, Y. *Polym. Eng. Sci.* **2008**, *48*, 912.
30. Rao, Y.; Waddon, A.; Farris, R. *Polymer* **2001**, *42*, 5937.
31. Ishida, H.; Wellinghoff, S. T.; Baer, E.; Koenig, J. L. *Macromolecules* **1980**, *13*, 826.
32. Ishida, H.; Huang, M. *J. Polym. Sci., Part B: Polym. Phys.* **1994**, *32*, 2271.
33. Shin, T. J.; Ree, M. *J. Phys. Chem. B* **2007**, *111*, 13894.
34. Shin, T. J.; Ree, M. *Langmuir* **2005**, *21*, 6081.
35. Morsy, M.; Al-Khaldi, M.; Suwaiyan, A. *J. Phys. Chem. A* **2002**, *106*, 9196.
36. Zhuang, Y.; Gu, Y. *J. Macromol. Sci. B* **2013**, *52*, 1603.
37. Wakita, J.; Jin, S.; Shin, T. J.; Ree, M.; Ando, S. *Macromolecules* **2010**, *43*, 1930.

38. Yin, C.; Dong, J.; Zhang, Z.; Zhang, Q.; Lin, J. *J. Polym. Sci., Part B: Polym. Phys.* **2014**.
39. Wu, T.-M.; Blackwell, J.; Chvalun, S. N. *Macromolecules* **1995**, *28*, 7349.
40. Wu, T.; Chvalun, S.; Blackwell, J.; Cheng, S.; Wu, Z.; Harris, F. *Acta Polym.* **1995**, *46*, 261.
41. Ran, S.; Fang, D.; Zong, X.; Hsiao, B.; Chu, B.; Cunniff, P. *Polymer* **2001**, *42*, 1601.
42. Kwei, T. *J. Polym. Sci.,Polym. Lett. Ed* **1984**, *22*, 307.
43. Liu, Y. L.; Hsu, C. W.; Chou, C. I. *J. Polym. Sci., Part A: Polym. Chem.* **2007**, *45*, 1007.
44. Su, Y.-C.; Chang, F.-C. *Polymer* **2003**, *44*, 7989.
45. Sukhanova, T.; Baklagina, Y. G.; Kudryavtsev, V.; Maricheva, T.; Lednický, F. *Polymer* **1999**, *40*, 6265.
46. Chen, S.; Hu, P.; Greiner, A.; Cheng, C.; Cheng, H.; Chen, F.; Hou, H. *Nanotechnology* **2008**, *19*, 015604.
47. Sen-biao, H.; Zhong-min, G.; Xiao-ye, M.; Hai-quan, G.; Xue-peng, Q.; Lian-xun, G. *Chem. Res. Chinese. U* **2012**, *28*, 752.
48. Ding, M. Polyimides: Chemistry, relationship between structure and properties and materials 21st Century SP's Series in Chemistry; Beijing; **2006**, p 571.